

Received September 5, 2019, accepted October 12, 2019, date of publication October 15, 2019, date of current version October 25, 2019.

Digital Object Identifier 10.1109/ACCESS.2019.2947533

Approximation Algorithm Based Channel Estimation for Massive MIMO Antenna Array Systems

HAO JIANG^{1,2}, (Member, IEEE), DENGHONG TANG³, JIE ZHOU^{1,2}, (Senior Member, IEEE),
XIAOLI XI³, JIAO FENG⁴, JIAN DANG⁵, (Member, IEEE), AND LIANG WU⁵, (Member, IEEE)

¹College of Artificial Intelligence, Nanjing University of Information Science and Technology, Nanjing 210044, China

²College of Electronic and Information Engineering, Nanjing University of Information Science and Technology, Nanjing 210044, China

³Institute of Advanced Navigation and Electromagnetics, Xi'an University of Technology, Xi'an 710048, China

⁴School of Electronic and Information Engineering, Nanjing University of Information Science and Technology, Nanjing 210044, China

⁵National Mobile Communications Research Laboratory, Southeast University, Nanjing 210096, China

Corresponding author: Jiao Feng (jiao.feng@nuist.edu.cn)

This work was supported in part by the National Key Research and Development Program of China under Grant 2018YFB1801101, in part by the National Natural Science Foundation of China under Grant 61971136, Grant 61601119, Grant 61771248, and Grant 61971167, in part by the Jiangsu NSF Project under Grant BK20191261, in part by the Fundamental Research Funds for the Central University, in part by the Major Program of the Natural Science Foundation of Institution of Higher Education of Jiangsu Province under Grant 14KJA510001, in part by the Startup Foundation for Introducing Talent of NUIST, and in part by the Priority Academic Program Development of Jiangsu Higher Education Institutions.

ABSTRACT This paper presents a three-dimensional (3D) massive multiple-input and multiple-output (MIMO) antenna array model, which includes the spherical array assumption and geometric properties for future fifth generation (5G) wireless communications. A parametric approximation algorithm is developed for estimating the spatial fading correlations (SFCs) and channel capacities of the 3D massive MIMO antenna array systems under different power angular spectrum (PAS). The relationship between correlation with the spacing of antenna arrays and angular parameters was classified. The results show that the simulation values of the approximate method fit the theoretical calculation very well, thereby validating the feasibility of the proposed 3D large-scale massive MIMO model.

INDEX TERMS Massive MIMO antenna array, spatial fading correlation, power Azimuth spectrum, approximation algorithm.

I. INTRODUCTION

Massive multiple-input and multiple-output (MIMO) technologies have been suggested as a promising technology in modern wireless communication systems [1]. The fifth generation (5G) wireless communication networks providing with more stable and high-speed wireless access services are expected to further improve user experience, which put forward higher requirements related to the artificial intelligence for MIMO key technologies [2]–[4]. It has been demonstrated that the scattering distribution and MIMO antenna structures and polarization employed have a critical impact on the MIMO channel performance. To establish more superior communication systems, one essential work is to investigate the channel characteristics for 5G massive MIMO channel models [5]. As the most fundamental channel

parameters, the spatial fading correlation (SFC) and channel capacity play an important role in the planning, evaluation, and optimization of massive MIMO wireless communication systems [6], [7].

Until now, many researchers have carried out works and modeling analysis of antenna arrays for the wireless transmission environment. References [8]–[11] proposed a series of MIMO planar antenna arrays, such as the uniform linear array (ULA), uniform circular array (UCA), uniform rectangular array (URA), and the L-shaped array configurations are proposed and investigated. The correlation-based traditional Kronecker models were demonstrated to help analyze the performance of compact MIMO systems [12]. Moreover, Mammassis presented the concept of Von-Mises-Fisher distribution in [13] and analyzed the SFC functions for the UCA antenna channels. Furthermore, in the 5G MIMO technology high-capacity evaluation, Zhou *et al.* [14] developed an electromagnetic vector sensor and applied it to

The associate editor coordinating the review of this manuscript and approving it for publication was Yue Cao ¹.

the deterministic covariance matrix of the MIMO uniform concentric circular array (UCCA) at the transmitter and receiver. Besides, the UCCA was compared with the ULA and UCA in the same channel model to demonstrate that the use of a UCCA can effectively reduce the dynamic range and system noise of the compensation filter which were generated in obtaining a large bandwidth range for the stable frequency using the UCA antennas [15]. Nevertheless, these array configurations are limited to 2D analyses and do not apply to general massive MIMO systems for the low spatial utilization and concern about antenna blockage from outer antennas.

As an important communication scenario, massive MIMO channel modeling has received more and more attention in recent years. The existing research has involved a series of typical power angular distributions such as the uniform, Gaussian and Laplacian distribution [16]. The authors in [17] derived the three-dimensional (3D) spatial correlation functions for the antenna systems using uniform concentric ring arrays (UCRAs) under a uniform angular distribution, which investigated the 3D spatial correlation for any two different elements located at any two rings of a UCRA. The authors in [18] proposed a generalized analytical expression for the spatial correlation function for the full dimension MIMO (FD-MIMO) channel constituted by UCAs of antenna ports at the base station and the mobile station. Furthermore, the authors in [19] researched the near-field effects and non-stationarity of the MIMO antenna arrays. However, they did not consider the impact of the spherical wavefront and the time-variant properties on the non-line-of-sight (NLoS) components. For massive MIMO communication systems, the authors in [20] presented a theoretical non-stationary wide-band twin-cluster channel model and time-variant and array-variant elliptical channel model, respectively. The time and frequency cross-correlation functions for every propagation component were analyzed; however, the angular spread of the incident signals in the elevation plane was not discussed in detail. Recently, a novel MIMO channel model with a 3D antenna array for congested curved-street vehicle-to-vehicle communication environments was presented in [21], in which the scatterers are located within narrow arcs along the curved street. The temporal and spatial cross-correlation functions corresponding to the single- and double-bounced scattering propagation paths were deduced; while the spatial fading correlations under different power angular spectrum (PAS) and channel capacities for the massive MIMO systems were not included. In the massive MIMO channel modeling, the traditional planar antenna array models cannot be applied directly, because of the changeable shape of mobile receivers and special communication environment [22].

In this paper, we present further analysis of a 3D massive MIMO antenna array model for future 5G wireless communications. A 3D spherical assumption is used in the proposed model, instead of the 2D planar wavefront assumption used in the traditional MIMO channel models. To evaluate the performance of the proposed 3D massive MIMO antenna arrays, we apply a parametric approximation algorithm for

the spatial fading correlations and the channel capacities of the 3D massive MIMO antenna arrays systems under different power azimuth spectrum. Besides, the applicability and computation time efficiency of the approximation algorithm are quantitatively analyzed considering the power spectrum PAS of indoor and outdoor environment, which provides an important theory for designing MIMO channels. The main contributions of this work are given as follows:

(1) We propose a 3D massive MIMO antenna array model with a spherical assumption for 5G wireless communication systems; works which have not been regularly found in the previous literature. The performance of the proposed antenna array model is analyzed in detail, including the impact of the antenna spacing on the spatial correlation between different antenna elements.

(2) We present a spherical wavefront assumption, instead of the plane wavefront assumption, to characterize the statistical proposition properties of massive MIMO communication systems. The impact of the spherical wavefront assumption on both the line-of-sight (LoS) and NLoS components in temporal and frequency domains are studied.

(3) A parametric approximation algorithm is employed in estimating the performance of the proposed massive MIMO antenna array model; the results show that the simulation results of the approximate method fit the theoretical calculation very well, which greatly improve the efficiency of analyzing and simulating large-scale massive MIMO communication systems.

(4) The SFCs and channel capacities of the proposed model are derived and investigated based on the parametric approximation algorithm; the simulation results provide theoretical guidance for the scattering distribution and antenna array layout of future massive MIMO channels in various indoor and outdoor testing scenarios.

The remainder of this paper is organized as follows: In Section II, the proposed 3D massive MIMO antenna model is discussed. Section III explains the parametric approximation algorithms for the SFCs and channel capacities of the 3D massive MIMO antenna arrays systems under different PAS. In Section IV, numerical results are presented and discussed. Finally, our conclusions are presented in Section V.

II. 3D MASSIVE MIMO ANTENNA ARRAY MODEL

A. SPHERICAL ARRAY ASSUMPTION

It is worth mentioning that the plane wavefront assumption is not fulfilled for 3D massive MIMO antenna array model [23]. This is because when we investigate the statistical propagation properties of massive MIMO channel model, it is improper to ignore the dimension of the antenna array [1]. Furthermore, the statistical propagation properties vary significantly over the large-scale antenna array. Therefore, we assume that the wavefront emitted from the interfering objects to the receiving array in the channel model is spherical. In this case, the angular parameters are no longer linear along the array. Instead, they must be computed based on the geometric relationships of the channel model [20].

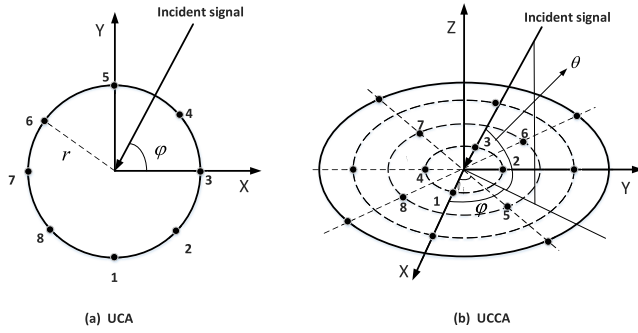


FIGURE 1. (a) Geometric uniform circular array; (b) Geometric uniform concentric circular array.

As introduced in [12], the UCA antenna array shown in Fig. 1(a) is not fulfilled for 5G massive MIMO technology high-capacity evaluation because the dynamic range and system noise of the compensation filter cannot be ignored. It is confirmed in [15] that the UCCA array antenna shown in Fig. 1(b) can effectively solve this problem. In this case, the signal spherical wavefront assumption is proposed, moreover, the channel impulse response of MIMO antenna arrays can be separated into steering-vector-dependent and time-dependent components [13], which can be expressed as

$$\mathbf{h}(t) = \sum_{p=1}^P a_p(t) \Psi(\Theta_p, \mathbf{g}_p) \quad (1)$$

where P denotes the number of large-scale antennas, $a_p(t)$ is one of a set of zero-mean complex independent identically distributed random variables, and $\Psi(\Theta_p, \mathbf{g}_p)$ is the steering vector of the compact antenna array in 3D space. The spatial vector parameters are given as $\Theta = [\theta, \varphi]^T$ and $\mathbf{g} = [\gamma, \eta]^T$. The scalars $0 \leq \varphi \leq 2\pi$ and $-\pi/2 \leq \theta \leq \pi/2$ denote the elevation and azimuth angles concerning the positive x - and z -axes, respectively. Moreover, the polarization phase difference and the auxiliary polarization angle are respectively denoted by the scalars $-\pi \leq \eta \leq \pi$ and $0 \leq \gamma \leq 2\pi$. Then under the assumption that the antenna elements are vertically polarized, we can express the steering vector of the UCCA in Fig. 1(b) as

$$\mathbf{a}(\theta, \varphi)_{UCCA} = [a_1(\theta, \varphi), a_2(\theta, \varphi), \dots, a_P(\theta, \varphi)]^T \quad (2)$$

where the superscript $[\cdot]^T$ stands for the transpose and $\mathbf{a}_p(\theta, \varphi)_{UCCA}$ is the phase delay at the p -th array element which can be expressed as

$$a_p(\theta, \varphi)_{UCCA} = \begin{cases} \exp \left\{ j2\pi \frac{r_p}{\lambda} \cos \left(\phi - \frac{2\pi(l-1)}{L} \right) \cos(\theta) \right\}, & \left[\frac{P}{L} \right] = 2k - 1, \quad k = 1, 2, 3 \dots \\ \exp \left\{ j2\pi \frac{r_p}{\lambda} \cos \left(\phi - \frac{\pi(2l-1)}{L} \right) \cos(\theta) \right\}, & \left[\frac{P}{L} \right] = 2k, \quad k = 1, 2, 3 \dots \end{cases} \quad (3)$$

where $l = 1, 2, \dots, p - \lfloor p/L \rfloor \times L, \dots, L$, r_p denotes the radius of the p -th array element and λ represents the signal wavelength.

The dimension attribute of the antenna array is expected to have a great impact on the overall channel performance. We herein introduce the large-scale omni-directional antenna array model including the spherical array assumption and geometric properties, as shown in Fig. 2.

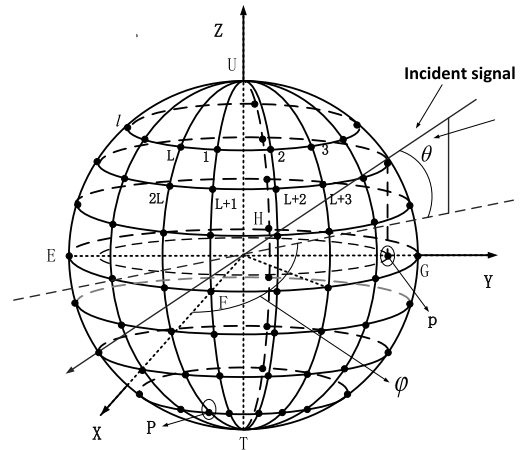


FIGURE 2. Proposed 3D massive MIMO antenna array.

B. SPACE AUTO-CORRELATION

Here in the proposed model, the omnidirectional spherical antennas receive signal wavefront emitted from the 3D clusters. We therefore present the whole antenna system as a 3D space spherical box. The antenna array elements are situated on the surface of in the spherical box, which constitutes the proposed 3D massive MIMO antenna array model. Furthermore, to realize the proposed 3D massive MIMO system, we number each antenna element according to the positions of each antenna element on the faces of the hemispheres, as shown in Fig. 2. In this case, the steering vector for the proposed array model can be expressed as

$$\mathbf{a}(\theta, \varphi) = \begin{bmatrix} e^{j\zeta \cos(\varphi - \varphi_1) \sin(\theta - \theta_1)}, e^{j\zeta \cos(\varphi - \varphi_2) \sin(\theta - \theta_2)}, \\ \dots, e^{j\zeta \cos(\varphi - \varphi_p) \sin(\theta - \theta_p)}, \\ \dots, e^{j\zeta \cos(\varphi - \varphi_P) \sin(\theta - \theta_P)} \end{bmatrix} \quad (4)$$

where the phase steering for the p -th element is denoted by $a_p(\theta, \varphi) = e^{j\zeta \cos(\varphi - \varphi_p) \sin(\theta - \theta_p)}$, $\zeta = 2\pi \frac{R}{\lambda}$, where R represents the radius of the spherical array. The azimuth and elevation angles concerning the x - and z -axes are respectively denoted by the scalars $0 \leq \varphi \leq 2\pi$ and $-\pi/2 \leq \theta \leq \pi/2$. Further, let us define V as the number of meridional rings and W as the number of zonal rings of the proposed vehicular antenna array model, therefore, the number of the large scale antennas $P = 2 \times V \times M$. According to the spherical upper and lower hemisphere array structure, the initial phase of the

p -th element can be expressed as

$$\begin{aligned} \varphi_p &= 2\pi \frac{l-1}{L}, \quad l = 1, 2, \dots, p - \left\lfloor \frac{p}{L} \right\rfloor \times L, \dots, L \quad (5) \\ \theta_p &= \frac{\pi}{W+1} \left(\frac{W+1}{2} - w \right), \quad w = 1, 2, \dots, \left\lceil \frac{p}{L} \right\rceil, \dots, W \quad (6) \end{aligned}$$

Please note that the expression in (2) assumes that the receive antennas are in the near field of the transmit antennas. Thus, the general space auto-correlation function with respect to the p -th and q -th elements can be defined as

$$\begin{aligned} \rho(p, q) &= \frac{E \left\{ (h_p - \tilde{h}_p)(h_q - \tilde{h}_q) \right\}}{\sqrt{E \left\{ (h_p - \tilde{h}_p)^2 \right\} E \left\{ (h_q - \tilde{h}_q)^2 \right\}}} \\ &= \frac{\int_{\varphi} \int_{\theta} \mathbf{a}_p(\theta, \varphi) \mathbf{a}_q^*(\theta, \varphi) \sin(\theta) f(\theta, \varphi) d\theta d\varphi}{\sqrt{\int_{\varphi} \int_{\theta} |\mathbf{a}_p(\theta, \varphi)|^2 \sin(\theta) f(\theta, \varphi) d\theta d\varphi}} \\ &\quad \times \frac{1}{\sqrt{\int_{\varphi} \int_{\theta} |\mathbf{a}_q(\theta, \varphi)|^2 \sin(\theta) f(\theta, \varphi) d\theta d\varphi}} \quad (7) \end{aligned}$$

where $E[\cdot]$ denotes the expectation, the superscript $(\cdot)^*$ is the complex conjugate, the scalar \tilde{h}_p is the mean value of the channel impulse response at antenna p , and the scalar $f(\theta, \varphi)$ is the joint probability density function (PDF) of the AoD of the multipath signal in 3D space.

III. APPROXIMATION ALGORITHM BASED CHANNEL CHARACTERISTICS

As described in [9], the analysis of channel correlations of the received signals by the antenna array in the three-dimensional domain also should be decomposed into the analysis of the azimuth and elevation angles. Furthermore, we assume that the elevation and azimuth angles are independent of each other [24], thus the function $f(\theta, \varphi)$ can be decomposed to $f(\theta)f(\varphi)$.

A. SPATIAL FADING CORRELATION UNDER UNIFORM DISTRIBUTION

For the proposed 3D large-scale arrays, we assume the incident signals are uniformly distributed in the elevation and azimuth planes, i.e., θ and φ are uniformly distributed over the range of angles $[\theta_M - \Delta_\theta, \theta_M + \Delta_\theta]$, and $[\varphi_M - \Delta_\varphi, \varphi_M + \Delta_\varphi]$. Δ_θ and Δ_φ are the elevation spread (ES) and azimuth spread (AS), respectively; θ_M and φ_M are the mean azimuth of arrival (MAOA) and mean elevation of arrival (MEOA), respectively. Therefore, the power azimuth spectrum functions can be expressed as

$$p(\varphi) = \frac{1}{2\Delta_\varphi}, \quad \varphi_M - \Delta_\varphi \leq \varphi \leq \varphi_M + \Delta_\varphi \quad (8)$$

$$p(\theta) = \frac{1}{2\Delta_\theta}, \quad \theta_M - \Delta_\theta \leq \theta \leq \theta_M + \Delta_\theta \quad (9)$$

From (7), the SFC between the antenna elements p and q of the proposed 3D array can be expressed as

$$\begin{aligned} \rho(p, q) &= G_1 \int_{\varphi_M - \Delta_\varphi}^{\varphi_M + \Delta_\varphi} \int_{\theta_M - \Delta_\theta}^{\theta_M + \Delta_\theta} \exp\{j2\pi \frac{R}{\lambda} [\cos(\varphi - \varphi_p) \\ &\quad \times \sin(\theta - \theta_p) - \cos(\varphi - \varphi_q) \sin(\theta - \theta_q)]\} \sin \theta d\theta d\varphi \\ &= G_1 \int_{\varphi_M - \Delta_\varphi}^{\varphi_M + \Delta_\varphi} \int_{\theta_M - \Delta_\theta}^{\theta_M + \Delta_\theta} \exp[j \sin \theta (Z_1 \cos \varphi \\ &\quad + Z_2 \sin \varphi) + j \cos \theta (Z_3 \cos \varphi + Z_4 \sin \varphi)] \sin \theta d\theta d\varphi \\ &= G_1 \int_{\varphi - \Delta_\varphi}^{\varphi + \Delta_\varphi} \int_{\theta_M - \Delta_\theta}^{\theta_M + \Delta_\theta} \exp[jZ_5 \sin \theta \sin \alpha \\ &\quad + jZ_6 \cos \theta \sin \beta] \sin \theta d\theta d\varphi \quad (10) \end{aligned}$$

where $G_1 = \sin \theta_M \sin \varphi_M / (4\Delta_\varphi \Delta_\theta)$, $\varphi = \varphi_M + \varepsilon + \gamma$, $Z_5 = \sqrt{Z_1^2 + Z_2^2}$, $Z_6 = \sqrt{Z_3^2 + Z_4^2}$, $\alpha = \varphi + \varepsilon$, $\beta = \varphi + \gamma$, and

$$Z_1 = 2\pi R/\lambda (\cos \varphi_p \cos \theta_p - \cos \varphi_q \cos \theta_q) \quad (11)$$

$$Z_2 = 2\pi R/\lambda (\sin \varphi_p \cos \theta_p - \sin \varphi_q \cos \theta_q) \quad (12)$$

$$Z_3 = 2\pi R/\lambda (\cos \varphi_q \sin \theta_q - \cos \varphi_p \sin \theta_p) \quad (13)$$

$$Z_4 = 2\pi R/\lambda (\sin \varphi_q \sin \theta_q - \sin \varphi_p \sin \theta_p) \quad (14)$$

$$\varepsilon = \tan^{-1}(Z_1/Z_2) \quad (15)$$

$$\gamma = \tan^{-1}(Z_3/Z_4) \quad (16)$$

We can further simplify (10) by making use of the well-known series [25], and the real and imaginary parts of $\rho(p, q)$ can be expressed as

$$\begin{aligned} \text{Re}\{\rho(p, q)\} &= G_1 \int_{\varphi - \Delta_\varphi}^{\varphi + \Delta_\varphi} \int_{\theta_M - \Delta_\theta}^{\theta_M + \Delta_\theta} [J_0(Z_5 \sin \theta + Z_6 \cos \theta) \\ &\quad + 2 \sum_{k=1}^{\infty} \{J_{2k}(Z_5 \sin \theta + Z_6 \cos \theta) \cos(2k\alpha) \cos(2k\beta)\}] \\ &\quad \times \sin \theta d\theta d\varphi \quad (17) \end{aligned}$$

$$\begin{aligned} \text{Im}\{\rho(p, q)\} &= G_1 \int_{\varphi - \Delta_\varphi}^{\varphi + \Delta_\varphi} \int_{\theta_M - \Delta_\theta}^{\theta_M + \Delta_\theta} 2 \sum_{k=1}^{\infty} \\ &\quad \times \sin [(2k+1)\alpha] \sin ((2k+1)\beta) \sin \theta d\theta d\varphi \\ &\quad \times J_{2k+1}(Z_5 \sin \theta + Z_6 \cos \theta) \quad (18) \end{aligned}$$

where $J_k(\cdot)$ is the Bessel function of k -th order and

$$J_\nu(Z) = \left(\frac{Z}{2}\right)^\nu \sum_{k=0}^{\infty} \frac{(-1)^k}{(k!) \Gamma(\nu + k + 1)} \left(\frac{Z}{2}\right)^{2k} \quad (19)$$

where $\Gamma(\cdot)$ is Gamma function, the series converges rapidly when values of Z become smaller. The use of these series should be satisfactory when considering antenna spacing up to several carrier wavelengths. Moreover, when assuming the

elevation spread Δ_θ and azimuth spread Δ_φ are small [26], we can obtain the spatial fading correlation approximation algorithm of the 3D massive MIMO antenna arrays under uniform distribution as

$$\begin{aligned} \text{Re}[\rho(p, q)] &= J_0(Z_5 \sin \theta + Z_6 \cos \theta) \\ &+ 2 \sum_{k=1}^{\infty} [J_{2k}(Z_5 \sin \theta + Z_6 \cos \theta) \\ &\times \cos(2k\alpha) \cos(2k\beta) \sin c(2k\Delta_\varphi) \sin c(2k\Delta_\theta)] \quad (20) \end{aligned}$$

$$\begin{aligned} \text{Im}[\rho(p, q)] &= 2 \sum_{k=0}^{\infty} [J_{2k+1}(Z_5 \sin \theta + Z_6 \cos \theta) \\ &\times \sin((2k+1)\alpha) \sin((2k+1)\beta) \\ &\times \sin c((2k+1)\Delta_\varphi) \sin c((2k+1)\Delta_\theta)] \quad (21) \end{aligned}$$

$$\begin{aligned} \rho(p, q) &\approx \exp(-j(Z_5 \sin \theta + Z_6 \cos \theta) \sin \alpha \sin \beta) \\ &\times \sin c((Z_5 \sin \theta + Z_6 \cos \theta) \cos \alpha \cos \beta \Delta_\varphi \Delta_\theta) \quad (22) \end{aligned}$$

B. SPATIAL FADING CORRELATION UNDER GAUSSIAN DISTRIBUTION

Secondly, if we assume that the azimuth and elevation θ and φ of incident signals follow the Gaussian angle energy distribution, respectively. The power azimuth spectrum functions can be expressed as

$$p(\varphi) = \frac{C_g}{\sqrt{2\pi}\sigma} \exp\left\{-\frac{(\varphi - \varphi_C)^2}{2\sigma^2}\right\} \quad (23)$$

$$p(\theta) = \frac{C_g}{\sqrt{2\pi}\sigma} \exp\left\{-\frac{(\theta - \theta_C)^2}{2\sigma^2}\right\} \quad (24)$$

where σ denotes the standard deviation of the Gaussian distribution, which is not related to the azimuth and elevation angle spreads in wireless channels [27]. The C_g is the normalization constant, θ_C and φ_C are the central azimuth of arrival (CAOA) and elevation of arrival (CEOA), respectively.

Then we can get the expression of the spatial fading correlation function between the two elements for our 3D spherical arrays under the Gaussian angular distribution with the same method in Section III.A, i.e.,

$$\begin{aligned} \rho(p, q) &= G_2 \int_{\varphi_M - \Delta_\varphi}^{\varphi_M + \Delta_\varphi} \int_{\theta_M - \Delta_\theta}^{\theta_M + \Delta_\theta} \exp\{j2\pi \frac{R}{\lambda} [\cos(\varphi - \varphi_p) \\ &\times \sin(\theta - \theta_p) - \cos(\varphi - \varphi_q) \sin(\theta - \theta_q)]\} \sin \theta d\theta d\varphi \\ &= G_2 \int_{\varphi_M - \Delta_\varphi}^{\varphi_M + \Delta_\varphi} \int_{\theta_M - \Delta_\theta}^{\theta_M + \Delta_\theta} \exp[j \sin \theta (Z_1 \cos \varphi + Z_2 \sin \varphi) \\ &+ j \cos \theta (Z_3 \cos \varphi + Z_4 \sin \varphi) - (\varphi - \varphi_C)^2 \\ &- (\theta - \theta_C)^2] \sin \theta d\theta d\varphi \end{aligned}$$

$$\begin{aligned} &= G_2 \int_{\varphi_M - \Delta_\varphi}^{\varphi_M + \Delta_\varphi} \int_{\theta_M - \Delta_\theta}^{\theta_M + \Delta_\theta} \exp[jZ_5 \sin \theta \sin \alpha + jZ_6 \cos \theta \sin \beta \\ &- (\varphi - \varphi_C)^2 - (\theta - \theta_C)^2] \sin \theta d\theta d\varphi \quad (25) \end{aligned}$$

where $G_2 = (1/2\pi\sigma^2) \sin \theta_M \sin \varphi_M$, Δ_θ and Δ_φ are the elevation spread (ES) and azimuth spread (AS), respectively; θ_M and φ_M are the mean azimuth of arrival (MAOA) and mean elevation of arrival (MEOA), respectively. It is worth mentioning that the definitions of Z_1 - Z_6 in (25) are the same as the ones in the derivations for uniform distribution in Section III.A. Similarly, when assuming the parameter σ is small, the spatial fading correlation of the 3D massive MIMO antenna arrays under Gaussian distribution can be approximately written as

$$\begin{aligned} \text{Re}[\rho(p, q)] &= J_0(Z_5 \sin \theta + Z_6 \cos \theta) \\ &+ 2 \sum_{k=1}^{\infty} \{J_{2k}(Z_5 \sin \theta + Z_6 \cos \theta) \cos(2k\alpha) \cos(2k\beta) \\ &\times \exp(-2\sigma^2 k^2) \text{Re}[\text{erf}(\frac{\pi + i2k\sigma^2}{\sqrt{2}})]\} \quad (26) \end{aligned}$$

$$\begin{aligned} \text{Im}[\rho(p, q)] &= 2 \sum_{k=0}^{\infty} \{J_{2k+1}(Z_5 \sin \theta + Z_6 \cos \theta) \sin((2k+1)\alpha) \\ &\times \sin((2k+1)\beta) \exp(-(2k+1)^2\sigma^2/2) \\ &\times \text{Re}[\text{erf}(\frac{\pi + i(2k+1)\sigma^2}{\sqrt{2}})]\} \quad (27) \end{aligned}$$

$$\begin{aligned} \rho(p, q) &\approx \exp(-j(Z_5 \sin \theta + Z_6 \cos \theta) \sin \alpha \sin \beta) \\ &\times \sin c((Z_5 \sin \theta + Z_6 \cos \theta) \cos \alpha \cos \beta \Delta_\varphi \Delta_\theta) \\ &\times \exp(-[(Z_5\sigma \cos \alpha)^2 + (Z_6\sigma \cos \beta)^2]/2) \quad (28) \end{aligned}$$

C. CHANNEL CAPACITY ANALYSIS

According to the results in [28], the channel capacity can comprehensively indicate the reception performances of the multiple antenna systems. Here we study the effect of approximation algorithms and array spatial orientation characteristics on the capacity of massive MIMO channel based on the fading spatial signal and power transmission characteristics. The instantaneous channel capacity of a stochastic MIMO channel under an average transmitting power constraint can be presented as:

$$C = \log_2 \left[\det \left(I_{N_r} + \frac{SNR}{N_t} HH^H \right) \right] \quad (29)$$

where $\det(\cdot)$ denotes a determinant, I_{N_r} is a $N_r \times N_r$ unit matrix and SNR denotes the channel signal-to-noise ratio. H denotes the $N_r \times N_t$ complex fading envelopes whose entries describe the channel response from the transmitter antenna to the receiver antenna. The h_{ij} entry of the channel

matrix represents the normalized channel transfer function evaluated at the frequency of operation between the transmitter antenna j and the receive antenna i . $[\cdot]^H$ denotes the conjugate transpose of a matrix. The channel capacity of stochastic MIMO channel corresponds to a random variable. For a MIMO receiving system with N_t transmit antennas and N_r receive antennas, the well-known iid assumption that the fades between pairs of transmit-receive antennas is independent and identical is not practical in many cases. In the spatial correlation MIMO channel, the channel transfer matrix H , entries generated by making use of the correlation information of the transmitting and receiving fading signals are given by:

$$H = R_r^{1/2} H_w R_t^{1/2} \tag{30}$$

The ergodic capacity of a MIMO channel is defined as the statistical mean value of the instantaneous capacity over the time delay. Hence:

$$E[C(t)] = E \left[\log_2 \left[\det \left(I_{N_r} + \frac{SNR}{N_t} H H^H \right) \right] \right] \tag{31}$$

where R_t and R_r are the covariance matrices of the transmitting and receiving antenna arrays of sizes $N_t \times N_t$ and $N_r \times N_r$. H_w denotes a $N_r \times N_t$ stochastic matrix with complex Gaussian independent identically distributed (iid) entries, and these entries describe the channel response from the transmitter antenna to the receiver antenna. We can numerically evaluate the capacity based on the spatial correlation matrix for the various antenna arrays by using the above equations in the proposed 3D channel model.

It can be obtained from the Jans inequality $E \log x \leq \log E x$ that

$$C \leq B \cdot \log_2 \left| I + \frac{\gamma_{ij}}{N} R \right| \tag{32}$$

where $R = E[H \cdot H^T]$, and the element γ_{ij} can be expressed by

$$\gamma_{ij} = \sum_{k=1}^N [h_{ij} \cdot h_{ij}^*] \tag{33}$$

where $*$ represents the complex conjugate. If we assume $\sigma_i = \sum_{j=1}^N |h_{ij}|^2 = \sum_{j=1}^N h_{ij} \cdot h_{ij}^* = 1$, the normalized correlation coefficient ρ_{ij} can be defined as

$$\rho_{ij} = \frac{1}{\sqrt{\sigma_i \sigma_j}} = \gamma_{ij} \tag{34}$$

It can be seen that the array signal fading correlation channel has a great influence on the massive MIMO channel capacity. The theoretical calculation and simulation experiments are used to obtain the approximations under certain conditions. Besides, the applicability of the approximate calculation method as well as the computational efficiency of massive MIMO arrays are quantitatively analyzed, which is of great significance for future research and innovation of new technologies.

IV. RESULTS AND DISCUSSION

Authors in [11]- [14] have studied a series of small-scale MIMO arrays according to the specific conditions of the mobile transmitter and receivers, such as UCA and UCCA models. Various MIMO array models have their characteristics, for example, omni-directional and unambiguous orientation information with the same array aperture from 0 to 2π are available when using a UCA symmetric array. Moreover, the use of a UCCA array can relieve the dynamic range and system noise of the compensation filter.

In this section, we focus on the analysis of the SFC and capacity approximation algorithm and its complexity of the array channel under different PAS distributions based on the proposed 3D massive MIMO model (seen in Fig. 2). The method can also be applied to analyze other future massive MIMO arrays by adjusting the channel parameters.

A. SPATIAL FADING CORRELATIONS

The accurate and approximate results of SFCs between array element 1 and 2 under the PAS uniform and Gaussian distribution are respectively depicted in Fig. 3 and Fig. 4. As the ring radius R of the array antenna increases, the spatial fading correlation SFC becomes smaller and gradually tends to zero. This is because that when the ring radius is larger, the array spacing or the angular distribution of the arrival signal becomes wider, and the interaction effect between the array elements becomes smaller. Furthermore, the SFCs descend faster and become smaller whit an increase in the PAS distribution angle spread. Also, Fig. 3 shows that while the PAS parameters $\Delta_\varphi = \Delta_\theta \geq 15^\circ$, the approximate analysis curve is almost coincident with the accurate curve when the normalized antenna spacing of the compact MIMO array $R/\lambda \leq 0.5$. However, as the radius of the array ring R increases, the approximate result will appear a certain deviation. When $\Delta_\varphi = \Delta_\theta \leq 5^\circ$, the approximate analysis and the accurate curves are almost coincident for any ring radius. We can also conclude from Fig. 4 that the overall

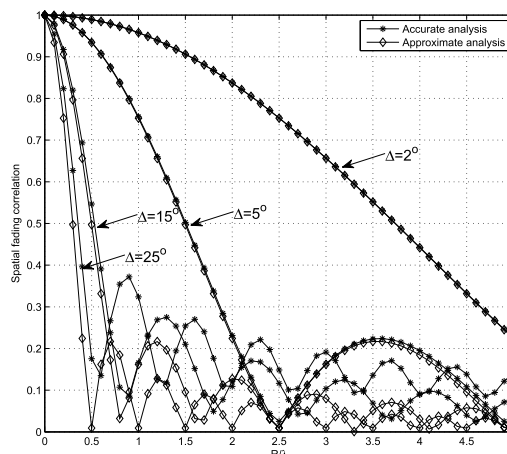


FIGURE 3. SFCs of the proposed 3D massive MIMO array model with uniformly distributed PAS ($\Delta = \Delta_\varphi = \Delta_\theta$).

TABLE 1. Running time of algorithms under different PAS distributions (unit: sec [s]).

PAS parameters	Uniform distribution		Gaussian distribution	
	Accurate calculation	Approximate calculation	Accurate calculation	Approximate calculation
σ				
2°	0.315170	0.000114	0.336909	0.000103
5°	0.311471	0.000115	0.330714	0.000112
15°	0.308066	0.000112	0.329841	0.000100
25°	0.316595	0.000116	0.326028	0.000107

TABLE 2. Channel capacity and running time of the massive MIMO arrays under different antenna number and power spectrum distribution (unit: sec [s]).

Massive MIMO antenna number	PAS distribution			
	Uniform distribution		Gaussian distribution	
	Accurate calculation	Approximate calculation	Accurate calculation	Approximate calculation
$m \times n$				
48×48	5.4167	0.0018	5.9743	0.0012
192×192	137.2421	0.0232	151.1573	0.0105
432×432	275666873	0.0470	296.6370	0.0216

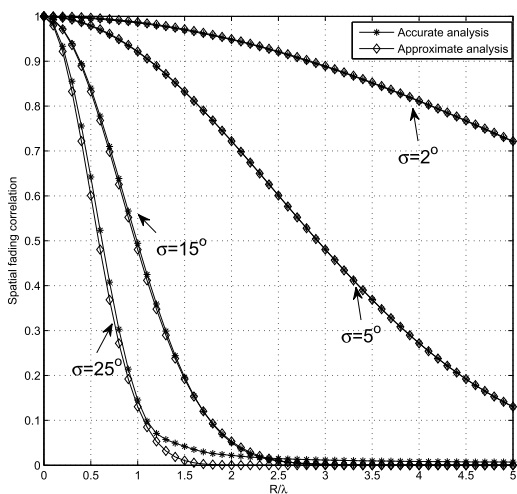


FIGURE 4. SFCs of the proposed 3D massive MIMO array model with PAS Gaussian distribution.

trend of the approximate result fits well with the accurate theoretical results within 15° .

Furthermore, the simulation results under large angular spread ($\Delta_\varphi = \Delta_\theta = \pi/3, \sigma = \pi/3$) are shown in Fig. 5. It can be observed that there is a big deviation

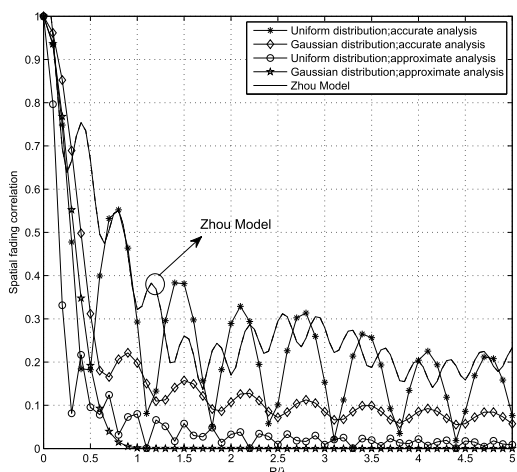


FIGURE 5. SFCs of the proposed 3D massive MIMO array model when $\Delta_\varphi = \Delta_\theta = \pi/3$ and $\sigma = \pi/3$.

when the PAS spreading angle is large and can fit well only if $R/\lambda \leq 0.25$, which is actually in line with the algorithm assumptions in Section 3. The fading trend shows good agreement with the simulation results in the Zhou model [14] for wireless communication scenarios. A conclusion can be made from the SFC results that the fading has periodic characteristics, so that low correlation nodes should be selected to increase polarization isolation and port isolation. Moreover, it is necessary to make full use of antenna diversity technology to maintain the independence of the signal and reduce the spatial factor of the MIMO array element in the designing of massive MIMO channels.

The use of trigonometric functions in array calculation could make the calculation more complex and take more CPU time. Testing by the DELL 3.5GHz work-station, the running time of the SFC algorithms under different PAS distributions for the proposed 3D massive MIMO antenna array model is given in Tab.1. Note that the approximation algorithm can save a considerable amount of time and have better efficiency and higher accuracy. In summary, when the PAS parameters are small, the approximate algorithm proposed in this paper can be well applied to analyze the proposed compact MIMO arrays. Moreover, it can greatly save computation time and improve numerical computation efficiency. The method can also be applied to the analysis of other future massive MIMO arrays used by the 5G systems.

B. MASSIVE MIMO CAPACITIES

For the massive MIMO array design analysis, the multi-dimensional array layout as Fig. 2 is used to obtain high-density antenna layout and performance. Here the number of the massive MIMO antenna elements is $P = 2 \times V \times M$, for further analysis, we set the number to $P = Q = 48; 192; 432$ (i.e., $V = 4, W = 6; V = 8, W = 12; V = 12, W = 18$), respectively. Fig. 6(a) and (b) show the channel capacity of the massive MIMO system with different array elements in the Gaussian and uniform distributions, respectively. It can be seen from the figure that as the signal-to-noise ratio and the number of array elements increase, the channel capacity increases sharply from the beginning, then grows slowly, and gradually tends to be stable and exhibits a non-linear growth relationship.

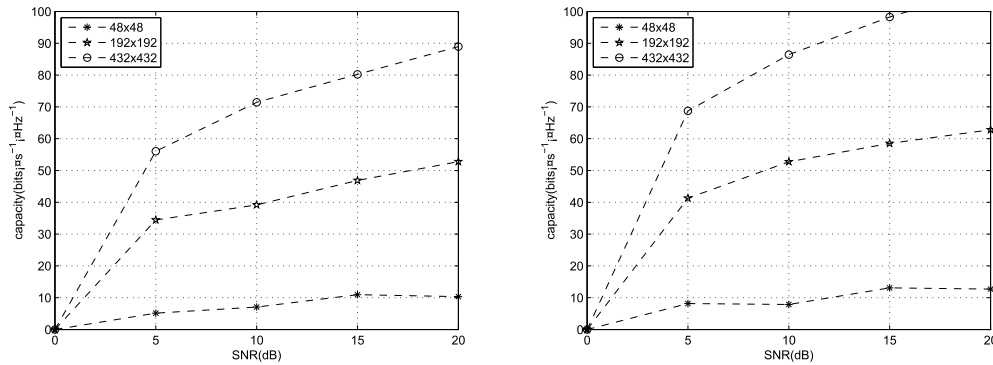


FIGURE 6. Inter channel capacity of the proposed 3D massive MIMO array model when $R/\lambda = 1$, $\varphi = 0^\circ$, $\sigma = 45^\circ$, $\theta_M = 45^\circ$, $\varphi_M = 30^\circ$, $\theta_C = 0$, $\varphi_C = 0$. (a) PAS uniform distribution; (b) PAS Gaussian distribution.

As the number of MIMO elements increases by 16 times and 81 times at $SNR = 10$ dB, the channel capacity under Gaussian distribution is slightly larger than that under the uniform distribution, which verifies that the array structure design has certain potential in improving MIMO performance. Tab.2 shows the approximate algorithm for calculating the channel capacity of massive MIMO array. The result shows that the approximation algorithm for the channel capacity can save considerable time and have good fitting and adaptability with the accurate calculation.

V. CONCLUSION

In this paper, we proposed a new 3D massive MIMO antenna array model for future 5G wireless communications. A 3D spherical assumption was used in the proposed model, instead of the 2D planar assumptions used in the traditional MIMO channel models. Furthermore, parametric approximation algorithm for the spatial fading correlations and channel capacities of the 3D massive MIMO antenna arrays systems under various angular energy distributions corresponding to the uniform and Gaussian distribution has been deduced. Also, simulations of the SFCs approximation algorithm and its complexity are analyzed. It was concluded that the deployment of antenna array spacing plays a decisive role in correlations between the angular spread of multi-path signals. The results show that the simulation values of the approximate method can fit the theoretical calculation very well and can save a lot of time for system simulations, thereby validating the applicability and feasibility of the proposed 3D large-scale massive MIMO model. The method can also be applied to the analysis of other future massive MIMO arrays. For future work, we will employ polarized antenna arrays and antenna lobe pattern analysis in the extensions of the proposed channel model.

REFERENCES

- [1] H. Jiang, Z. Zhang, J. Dang, and L. Wu, "A novel 3-D massive MIMO channel model for vehicle-to-vehicle communication environments," *IEEE Trans. Commun.*, vol. 66, no. 1, pp. 79–90, Jan. 2018.
- [2] H. Huang, Y. Song, J. Yang, G. Gui, and F. Adachi, "Deep-learning-based millimeter-wave massive MIMO for hybrid precoding," *IEEE Trans. Veh. Technol.*, vol. 68, no. 3, pp. 3027–3032, Mar. 2019.
- [3] K. Kim, J. Lee, and J. Choi, "Deep learning based pilot allocation scheme (DL-PAS) for 5G massive MIMO system," *IEEE Commun. Lett.*, vol. 22, no. 4, pp. 828–831, Apr. 2018.
- [4] S. Kumar, K. Singh, S. Kumar, O. Kaiwartya, Y. Cao, and H. Zhou, "Delimitated anti jammer scheme for Internet of vehicle: Machine learning based security approach," *IEEE Access*, vol. 7, pp. 113311–113323, 2019.
- [5] H. Jiang, Z. Zhang, L. Wu, J. Dang, and G. Gui, "A 3-D non-stationary wideband geometry-based channel model for MIMO vehicle-to-vehicle communications in tunnel environments," *IEEE Trans. Veh. Technol.*, vol. 68, no. 7, pp. 6257–6271, Jul. 2019.
- [6] F. Cheng, G. Gui, N. Zhao, F. R. Yu, Y. Chen, J. Tang, and H. Sari, "Caching UAV assisted secure transmission in small-cell networks," in *Proc. Int. Conf. Comput., Netw. Commun.*, Mar. 2018, pp. 696–701.
- [7] M. Tian, J. Zhang, Y. Zhao, L. Yuan, J. Yang, and G. Gui, "Switch and inverter based hybrid precoding algorithm for mmWave massive MIMO system: Analysis on sum-rate and energy-efficiency," *IEEE Access*, vol. 7, pp. 49448–49455, 2019.
- [8] L. Wood and W. S. Hodgkiss, "Understanding the Weichselberger model: A detailed investigation," in *Proc. IEEE Mil. Commun. Conf.*, Nov. 2008, pp. 1–7.
- [9] S. K. Yong and J. S. Thompson, "Three-dimensional spatial fading correlation models for compact MIMO receivers," *IEEE Trans. Wireless Commun.*, vol. 4, no. 6, pp. 2856–2869, Nov. 2005.
- [10] F. Harabi, A. Gharsallah, and S. Marcos, "Three-dimensional antennas array for the estimation of direction of arrival," *IET Microw., Antennas Propag.*, vol. 3, no. 5, pp. 843–849, Aug. 2009.
- [11] D. Tang, G. Shao, Z. Jie, and H. Kikuchi, "A novel MIMO channel model for vehicle-to-vehicle communication system on narrow curved-road environment," *Wireless Pers. Commun.*, vol. 98, no. 4, pp. 3409–3430, 2018.
- [12] J.-H. Lee and S.-I. Li, "Spatial correlation characteristics of antenna systems using uniform concentric ring arrays," in *Proc. 16th Int. Conf. Digit. Signal Process.*, Jul. 2009, pp. 1–6.
- [13] K. Mammassis, R. W. Stewart, and J. S. Thompson, "Spatial Fading Correlation model using mixtures of Von Mises Fisher distributions," *IEEE Trans. Wireless Commun.*, vol. 8, no. 4, pp. 2046–2055, Apr. 2009.
- [14] J. Zhou, H. Jiang, and K. Hisakazu, "Performance of uniform concentric circular arrays in a three-dimensional spatial fading channel model," *Wireless Pers. Commun.*, vol. 83, no. 4, pp. 2949–2963, 2015.
- [15] S. C. Chan and H. H. Chen, "Uniform concentric circular arrays with frequency-invariant characteristics—Theory, design, adaptive beamforming and DOA estimation," *IEEE Trans. Signal Process.*, vol. 55, no. 1, pp. 165–177, Jan. 2007.
- [16] H. Jiang, Z. Zhang, and G. Gui, "Three-dimensional non-stationary wideband geometry-based UAV channel model for A2G communication environments," *IEEE Access*, vol. 7, pp. 26116–26122, 2019.
- [17] J.-H. Lee and S.-I. Li, "Three-dimensional spatial correlation characteristics of concentric ring antenna array systems," in *Proc. 17th Int. Conf. Digit. Signal Process.*, Jul. 2011, pp. 1–6.
- [18] Q.-U.-A. Nadeem, A. Kammoun, M. Debbah, and M.-S. Alouini, "Performance analysis of compact FD-MIMO antenna arrays in a correlated environment," *IEEE Access*, vol. 5, pp. 4163–4178, 2017.

- [19] S. Wu, C. X. Wang, and E. Aggoune, "Non-stationary wideband channel models for massive MIMO systems," in *Proc. WSCN*, Jeddah, Saudi Arabia, 2013, pp. 1–8.
- [20] S. Wu, C.-X. Wang, H. Haas, E. H. M. Aggoune, M. M. Alwakeel, and B. Ai, "A non-stationary wideband channel model for massive MIMO communication systems," *IEEE Trans. Wireless Commun.*, vol. 14, no. 3, pp. 1434–1446, Mar. 2015.
- [21] D. Tang, X. Xi, and J. Zhou, "A novel MIMO channel model for congested communication environments," *IEEE Access*, vol. 7, pp. 53754–53765, 2019.
- [22] Z. Zhang, Y. Liang, W. Shi, L. Yuan, and G. Gui, " $\ell_{1/2}$ -regularization-based super-resolution sparse channel estimation for MmWave massive MIMO systems," *IEEE Access*, vol. 7, pp. 75837–75844, 2019.
- [23] S. Wu, C.-X. Wang, E.-H. M. Aggoune, M. M. Alwakeel, and Y. He, "A non-stationary 3-D wideband twin-cluster model for 5G massive MIMO channels," *IEEE J. Sel. Areas Commun.*, vol. 32, no. 6, pp. 1207–1218, Jun. 2014.
- [24] Q.-U.-A. Nadeem, A. Kammoun, M. Debbah, and M.-S. Alouini, "A generalized spatial correlation model for 3D MIMO channels based on the Fourier coefficients of power spectrums," *IEEE Trans. Signal Process.*, vol. 63, no. 14, pp. 3671–3686, Jul. 2015.
- [25] J. Salz and J. H. Winters, "Effect of fading correlation on adaptive arrays in digital mobile radio," *IEEE Trans. Veh. Technol.*, vol. 43, no. 4, pp. 1049–1057, Nov. 1994.
- [26] A. Forenza, D. J. Love, and R. W. Heath, Jr., "Simplified spatial correlation models for clustered MIMO channels with different array configurations," *IEEE Trans. Veh. Technol.*, vol. 56, no. 4, pp. 1924–1934, Jul. 2007.
- [27] J. Zhou, S. Sasaki, S. Muramatsu, and H. Kikuchi, "Spatial correlation functions for a circular antenna array and their applications in wireless communication systems," *IEICE Trans. Fundam. Electron., Commun. Comput. Sci.*, vols. E86–A, no. 7, pp. 1716–1723, 2003.
- [28] H. Jiang, Z. Zhang, and G. Gui, "A novel estimated wideband geometry-based vehicle-to-vehicle channel model using an AoD and AoA estimation algorithm," *IEEE Access*, vol. 7, pp. 35124–35131, 2019.



JIE ZHOU received the B.S. and M.S. degrees in radio engineering from the Nanjing University of Posts and Telecommunications, Nanjing, China, in 1985 and 1990, respectively, and the Ph.D. degree in information engineering from Gunma University, Maebashi, Japan, in 2001. He is currently a Professor with the Nanjing University of Information Science and Technology, Nanjing. His current research interests include mobile communication theory and applications, radio access networks, and wireless sensor networks.



XIAOLI XI received the B.S. degree in applied physics from the University of Defense Technology, Changsha, China, in 1990, the M.S. degree in biomedical engineering from Fourth Military Medical University, Xi'an, China, in 1998, and the Ph.D. degree in electrical engineering from Xi'an Jiaotong University, Xi'an, China, in 2004. She is currently a Professor with the Department of Electric Engineering, Xi'an University of Technology, Xi'an. Her recent research interests include wave propagation, antenna design, and communication signal processing.



JIAO FENG received the B.Eng. and M.Sc. degrees in communications engineering from Jilin University, Jilin, China, in 2007 and 2009, respectively, and the Ph.D. degree in wireless communications from Southampton University, U.K., in 2014. Since 2014, she has been with the School of Electric and Information Engineering, Nanjing University of Information Science and Technology, China. She is involved in the projects sponsored by the National Natural Science Foundation and the Natural Science Foundation of Jiangsu Province. Her research interests include cooperative communication, network protocols, digital signal processing, cognitive radio networks, matching theory, machine learning, and natural language processing.



JIAN DANG (M'15) received the B.S. degree in information engineering and the Ph.D. degree in information and communications engineering from Southeast University, Nanjing, China, in July 2007 and September 2013, respectively. From September 2010 to March 2012, he was a Visiting Scholar with the Department of Electrical and Computer Engineering, University of Florida, USA. Since September 2013, he has been with the National Mobile Communications Research Laboratory, Southeast University. He is currently an Associate Professor. His research interests include signal processing in wireless communications and optical mobile communications.



LIANG WU received the B.S., M.S., and Ph.D. degrees from the School of Information Science and Engineering, Southeast University, Nanjing, China, in 2007, 2010, and 2013, respectively. From September 2011 to March 2013, he was a Visiting Ph.D. Student with the School of Electrical Engineering and Computer Science, Oregon State University. In September 2013, he joined the National Mobile Communications Research Laboratory, Southeast University. He is currently an Associate Professor. His research interests include optical wireless communications, multiple-input and multiple-output technology, interference alignment, and wireless indoor localization.

• • •



HAO JIANG (M'19) received the B.S. and M.S. degrees in electrical and information engineering from the Nanjing University of Information Science and Technology, Nanjing, China, in 2012 and 2015, respectively, and the Ph.D. degree from the National Mobile Communications Research Laboratory, Southeast University, Nanjing, in 2019. From 2017 to 2018, he was a Visiting Student with the Department of Electrical Engineering, Columbia University, New York, NY, USA. Since April 2019, he has been a Professor with the School of Information Science and Engineering, Nanjing University of Information Science and Technology. His current research interests include the general areas of vehicle-to-vehicle communications, massive multiple-input and multiple-output channel modeling, signal processing, communications, machine learning, and AI-driven technologies.



DENGHONG TANG received the B.S. and M.S. degrees in electrical and information engineering from the Nanjing University of Information Science and Technology, Nanjing, China, in 2013 and 2018, respectively. He is currently pursuing the Ph.D. degree with the Institute of Advanced Navigation and Electromagnetics, Xi'an University of Technology, Xi'an, China. His current research interests include the general areas of vehicle-to-vehicle communications, massive multiple-input and multiple-output channel modeling, and signal processing.